doi: 10.34248/bsengineering.1695801



Research Article

Volume 8 - Issue 5: 1429-1439 / September 2025

ANALYSING THE CHANGE OF ABOVEGROUND BIOMASS DENSITY USING EARTH OBSERVATION AND MACHINE LEARNING TECHNOLOGY: ALANYA CASE

Ercüment AKSOY1*

¹Akdeniz University, Technical Sciences Vocational School, Technical Sciences Vocational School, Department of Geographical Informations Systems, 07070, Antalya, Türkiye

Abstract: Aboveground biomass (AGB) is a key parameter in assessing forest carbon stocks, ecosystem productivity, and the global carbon cycle. This study aims to model the annual AGB change between 2019 and 2024 in Alanya, Türkiye, using remote sensing (RS) technologies and open-source datasets. Sentinel-2 surface reflectance data, slope data derived from the Copernicus GLO-30 Digital Elevation Model (DEM), and GEDI L4A biomass data were utilized. As GEDI point data cannot be directly used for mapping, it was employed as a reference for model training. Spectral bands and vegetation indices from Sentinel-2 imagery were modeled using the Random Forest algorithm. Model performance was evaluated using the coefficient of determination (R²) and root mean square error (RMSE). The highest total AGB was observed during the 2022–2023 period, while the lowest occurred between 2019–2020. The findings indicate that biomass dynamics in the region are influenced not only by climatic conditions but also significantly by anthropogenic activities. The study presents a remote sensing-based approach to support carbon-neutral strategies through accurate biomass monitoring.

Keywords: Geographic information systems, Remote sensing, Earth observation, Biomass, Above ground biomass (AGB)

*Corresponding author: Akdeniz University, Technical Sciences Vocational School, Technical Sciences Vocational School, Department of Geographical Informations Systems, 07070, Antalya, Türkiye

E mail: ercumentaksoy@akdeniz.edu.tr (E. AKSOY)

Ercüment AKSOY https://orcid.org/0000-0001-7313-0891

Received: May 09, 2025 Accepted: July 28, 2025 Published: September 15, 2025

Cite as: Aksoy E. 2024. Analysing the change of aboveground biomass density using earth observation and machine learning technology: Alanya case. BSJ Eng Sci, 8(5): 1429-1439.

1. Introduction

Although there are many definitions of biomass, it generally refers to the mass of plant organisms that grow and develop by photosynthesis per unit area. Biomass, which is formed as a result of plants storing solar energy by converting it into chemical energy through photosynthesis, is also considered as organic carbon for this reason (Kim et al., 2004).

Forest biomass is an important raw material for building materials, pulp and paper production and energy production as fuel. However, forests are also recognised as an important regulator of the world's climate because they capture and store large amounts of carbon in their woody biomass (De et al., 2025).

Forest ecosystems provide many goods and services to society when planned and managed sustainably. Forests have many economic functions as well as important ecological and environmental functions such as climate regulation, water conservation, soil conservation and biodiversity conservation. Recently, high consumption of fossil fuels, deforestation and changes in land use and land cover have caused serious changes in the atmosphere resulting in climate change and global

warming all over the world. Forest ecosystems store CO² in their biomass and in the soil for a longer period of time in the context of mitigating global climate change (Evrendilek et al., 2004). Forest ecosystems are an important component of the global carbon budget in terrestrial ecosystems and there is a need to accurately determine the amount of carbon they store (Sharma et al., 2008). Biomass estimation is crucial for determining carbon budgets (Güverçin, 2022). For this purpose, many methods are used to determine the biomass in a spesific area (Ravindranath and Ostwald, 2007).

Originating from the United Nations Framework Convention on Climate Change (UNFCCC), the Kyoto Protocol sets legally binding targets for industrialized countries to reduce their greenhouse gas emissions or remove them from the atmosphere. The Protocol was adopted in 1997 and finally entered into force in February 2005. The protocol aimed to reduce overall greenhouse gas emissions by at least 5 per cent below current 1990 levels during the commitment period from 2008 to 2012. To achieve this, industrialized member states have set different binding targets ranging from -8% to +10% of 1990 emissions. The EU has set a 'bubble'



target of -8 per cent by 2010 and -20 per cent by 2020, redistributed based on the EU agreement (UNFCCC). The UK's reduction target is set at 20 per cent below 1990 levels by 2010, with a further legally binding reduction target of 26-32 per cent below 1990 levels for 2020. In the face of growing concerns that national $\rm CO^2$ emission reduction targets cannot be met by emission reduction strategies alone, industrialised countries are keen to find alternative ways to reduce atmospheric $\rm CO^2$ concentrations.

An important mechanism for removing CO² from the atmosphere is carbon sequestration in growing vegetation. The Clean Development Mechanism (CDM) initiative under the Kyoto Protocol, among other things, envisages forestry projects for carbon sequestration. This allows industrialized countries to offset atmospheric carbon emissions by financing such projects in developing countries.

However, the viability of carbon sequestration programmers relies on both a scientific understanding of how CO^2 is captured and stored as vegetative biomass and the development of operational techniques to measure standing biomass globally.

The largest impact on the global carbon cycle comes from human activities through the burning of biomass and fossil fuels and extraction of vegetation, especially forests (Watson et al., 2000). It is estimated that about 75% of CO2 emissions to the atmosphere are from combustion, with the remainder contributed by land use change through the removal of carbon sinks (Prentice et al., 2001). It is therefore regrettable that the CDM currently excludes tropical forest conservation projects. Ongoing discussions culminated at the UN Climate Change Conference in Bali (COP 13 December 2007) with a call for the future inclusion of Reduced Emissions from Deforestation in Developing Countries (REDD), now commonly referred to as Reduced Emissions from Deforestation and Degradation. Therefore, in addition to estimating global forest biomass, forest monitoring is needed by quantifying deforestation and other potential sources of atmospheric CO² emissions, such as fire damage from forest areas. Earth observation techniques are ideal for such mapping and monitoring activities as they offer the ability to repeat data capture frequently and cover large areas that may be difficult to reach for field measurements.

With the increasing importance of forestry-based carbon sequestration initiatives and global forest monitoring, there is a need for accurate information at regional and national scales on the spatial extent, condition, biomass and growth potential of forests and woodlands with canopy cover as low as 10 per cent. Earth observation (EO) techniques are more suitable for biomass estimation than traditional in situ methods. The latter involves laborious fieldwork, often based on destructive sampling (Gilreath et al., 1994). While regional biomass estimates based on in situ methods are unlikely to accurately depict the heterogeneity of the landscape,

those based on EO data produce updatable biomass estimates that more accurately represent the spatial heterogeneity of the landscape. Depending on spatial and temporal resolution, EO can detect differences in the spatial distribution of biomass density, such as the occurrence of forest gaps and land cover changes and provides systematic observations at scales ranging from local to global while improving monitoring of inaccessible areas (Aaslyng et al., 2003).

Accurate land cover mapping from EO data combined with known biomass estimates for each land cover class is a relatively simple use of EO for biomass estimation. RadarRI methods such as Synthetic Aperture Radar (SAR) interferometry (InSAR) used for canopy height retrieval in closed canopy forests can be used in combination with allometric equations to estimate AG biomass (Askne et al., 1997). In addition, SAR backscattering has been statistically correlated with forest biomass up to a certain level depending on the radar wavelength (Le et al., 1992).

The most accurate and reliable methods for estimating above-ground biomass are terrestrial measurements. The above-ground biomass is accurately estimated using allometric equations obtained with the help of terrestrial data. This method is time consuming, labour intensive and difficult to implement. It is especially difficult to do in large areas (Lu et al., 2005). Biomass estimation with GIS is not a widely used method because it requires a large, accurate, reliable database and quality relationships between these data. Remote sensing method is preferred for estimating above-ground biomass especially in hardto-reach areas due to the ease of data collection, rapid data evaluation, high correlations between band brightness values, vegetation indices and texture values (Nelson et al., 1988; Sader et al., 1989; Franklin and Hiernaux, 1991; Steininger, 2000; Foody et al., 2001; Santos et al., 2003; Zheng et al., 2004).

The above-ground forest biomass potential (carbon stock) is classically calculated on the basis of values obtained from field measurements. An alternative method to this labour-intensive and time-consuming method should be estimated with the support of Geographic Information Systems (GIS) and Remote Sensing (RS) techniques, which provide a new and efficient approach. RS is based on the qualitative and quantitative evaluation of electromagnetic radiation emitted or reflected from an object without a mechanical connection and the remote detection and measurement of the properties of the object (Khan et al., 2024). Thanks to RS techniques, the earth and earth objects can be imaged by means of measuring instruments placed on platforms in the atmosphere or space at a certain distance from the earth (Al, 2022).

Developments in the field of RS have opened a new and efficient way to estimate forest biomass. Pixel-based and object-based (segmentation) image classification techniques, which are performed to interpret the images produced by RS techniques and to obtain information

from these images, provide faster and more practical results than approaches such as field measurement. The increase in image resolution in RS gives more importance to segmentation methods together with pixel-based classification techniques.

Recently, studies have been carried out to estimate above-ground biomass in large forested areas using remote sensing data (Houghton et al., 2009; Gallaun et al., 2010). In particular, Landsat satellite images, the first natural resource satellite, are used both in small areas and in large forested areas. However, there are many studies in the literature on estimating aboveground biomass using different satellite images (Muukkonen and Heiskanen, 2005; Eckert et al., 2012). Moreover, studies have also been carried out on the estimation of AGB using radar and lidar data, and it is stated that the model estimation results obtained from these studies give better results than the model estimation results obtained from optical satellite images (Lu et al., 2005; Houghton et al., 2009).

Lidar and radar satellite data have been used to estimate AGB in different forest ecosystems (Zhao et al., 2016; Keleş et al., 2024). It has been stated that especially long wavelength radar data can be used to estimate AGB in mixed forest ecosystems (Zimble et al., 2003).

A preliminary research study was carried out using the bibliometric analysis technique based on quantitative data and numerical measurement indicators of previous studies on the subject of biomass and Earth Observation technology including remote sensing and GIS technology. After searching for "earth observation" and "biomass" on Web of Science, Martin Herold was detected as the most cited author with 592 citations, Ian Mccallum with 527 citations, and A. Uwe Schneider with 510 citations.

When countries are considered in terms of the criteria of publishing at least 1 work and receiving 1 citation, the countries with the most citations are the USA (7513 citations), the UK (6590 citations) and Germany (5017 citations). In terms of total connectivity, two of these three countries are in the top three. The other country in the top three in terms of connectivity and in third place is Canada. In terms of the number of works, the ranking is England (151 publications), America (126 publications) and China (122 publications). These results are shown in the Figure 1. Citation Links of Countries below

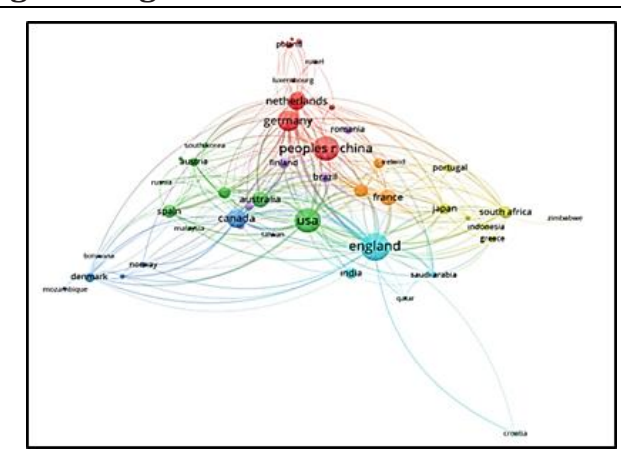


Figure 1. Citation links of countries.

Institutional structures make the most important contributions to biomass and Earth observation studies. In order to examine the work of institutions in the field and to identify institutions that are intensively active, the criteria of at least 1 work being published and 1 citation being received were examined. While the Chinese Academy of Sciences (45 works), Plymouth Marine Laboratory (33 works), and University of Leicester (28 works) were represented by works, the institutions addressing the most cited publications were the Chinese Academy of Sciences (1211 citations), the National Oceanic and Atmospheric Administration (1194 citations), and Plymouth Marine Laboratory (1081 citations). This institutional citation link relationship is shown in Figure 2. Citation Links of Institutions.

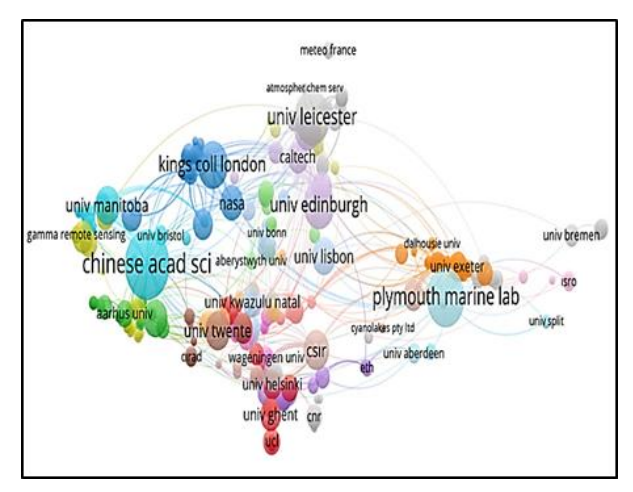


Figure 2. Citation links of institutions.

When we look at the most frequently used keywords in biomass and Earth observation publications, the most frequently used expressions are remote sensing (ground tracking) with 60 repetitions, lidar (sensor) with 35 repetitions, sentinel-2 (satellite) with 32 repetitions, modus (a type of radiometer developed by NASA) with 23 repetitions and phytoplankton (photo-plankton) with 20 repetitions. This keyword link information is shown in Figure 3. Most Frequently Used Keyword links below.

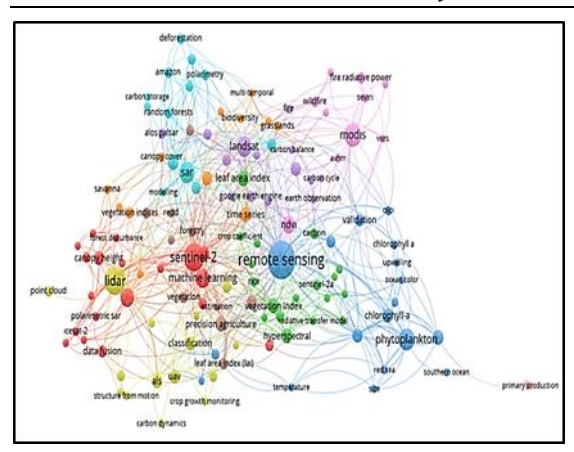


Figure 3. Most Frequently Used Keyword Links

In biomass studies, total Aboveground Biomass (AGB) data are primarily derived from GEDI observations. Utilizing laser technology, GEDI maps vegetation in the vertical dimension, enabling three-dimensional modeling of biomass distribution, particularly in tropical and temperate forest ecosystems (Duncanson et al., 2022). The mission has been instrumental in tracking annual forest carbon changes at a spatial resolution of 1 km (Potapov et al., 2021). In the Amazon Basin, combining GEDI data with Sentinel-2 satellite imagery has achieved high biomass estimation accuracy, reaching up to 82%. This accuracy has been further enhanced in steep and densely forested areas (Silveira et al., 2023). Similarly, GEDI-based validation studies in western U.S. forests have yielded strong correlation coefficients ($R^2 = 0.90$) and low error rates (RMSE = 32.62 Mg/ha) (Cao et al., 2023). Comparable results have also been reported in boreal forests in Norway.

This study proposes a high-accuracy biomass estimation methodology based on remote sensing and open-access datasets. The integration of image processing techniques and index-based models allows for rapid and precise analysis over large areas. The use of publicly available data not only minimizes operational costs but also enhances sustainability by enabling frequent analysis and retrospective access to long-term time series datasets. These aspects represent major advantages of the proposed approach in supporting data-driven forest carbon monitoring.

2. Materials and Methods

Study Area Alanya. 36'30'07' and 36'36'31' north latitudes and 31'38'40' and 32'32'02' east longitudes, 135 km from the city centre within the borders of Antalya province on the Mediterranean coast of Türkiye. The study area is shown in the following Figure 4.

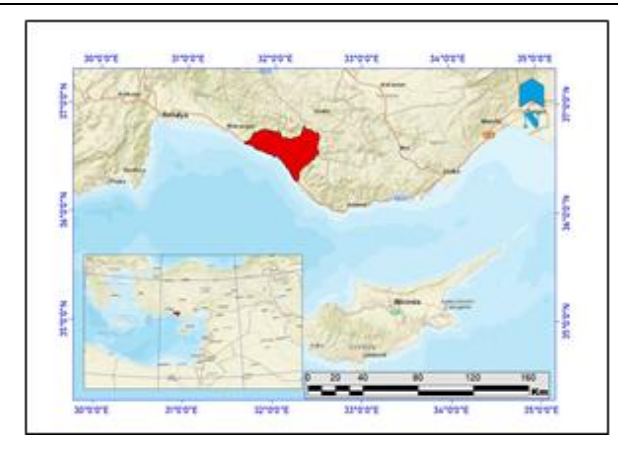


Figure 4. Geolocation.

Alanya district, which is the study area, is the district with the most fertile soil richness of the region due to its location and climate characteristics. District forests account for 0.5% of Türkiye's forest size. Afforestation works are carried out in the region. An average area of 750 hectares is afforested annually.

While the mountainous areas of the region have larch and cedar trees, the coastal areas have red pine tree type. Due to banana and citrus production, which brings significant income to the region, these tree types are intensively present (Turgut and Günlü, 2022). These trees are generally located in the coastal area. While Avacado and Kiwi trees can be observed in every area, Ouince, Pear and Apple trees are found in mountainous areas due to their cold resistance. Recently, as a result of the planting of Eucalyptus trees as a method in the marsh drying works, these types of trees are found in the region for ornamental purposes. As can be seen in the light of the above information, the region contains a rich green area type due to its different characteristics. The green area information of the study area is given in the area and percentage information with the Pie Slice Image in Figure 5.

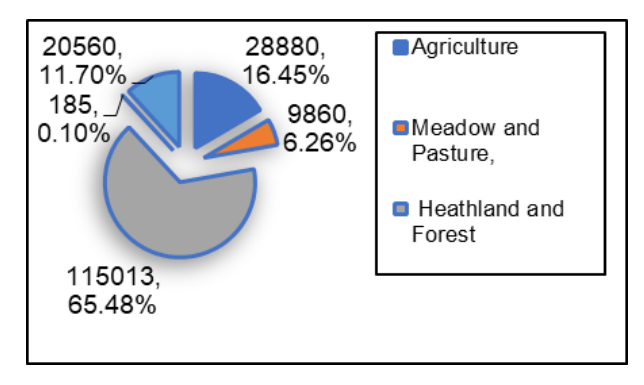
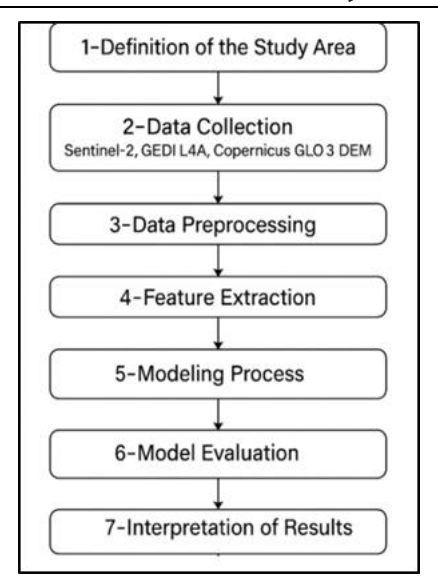


Figure 5. Green area information (Alanya Governorship). All procedures carried out in the study were itemized and presented in the form of a workflow diagram. The flowchart is shown in the following Figure 6.



Climatically, when the study area is examined, the region has arid and hot summers. It has been determined that the winters are rainy and mild. The breeze wind coming from the sea reduces the heat effect in summer. Table 1 below, contains information that helps to deduce the average climatic characteristics of the province where the study area is located between 1930 and 2024.

17.05.2020 measurement was determined as 41.7 $^{\circ}$ C, 06.06.2000 measurement was determined as 45 $^{\circ}$ C, 01.10.2022 measurement was determined as 41.2 $^{\circ}$ C and 06.06.2024 measurement was determined as 45 $^{\circ}$ C. For the generation of climate data, 30-year data of 220 stations were used.

Figure.6. Flowchart.

Table.1. Average climatic characteristics between 1930 and 2023

Month	АТ	АНТ	AMT	AST	ANRD	MTRA	1930 - 2023	
							*HT (°C)	*LT (°C)
1	10	14.9	6	5.1	12.5	234.5	23.9	-4.3
2	10.7	15.6	6.4	5.8	10.45	150.2	26.7	-4.6
3	12.9	18	8.1	6.7	8.63	92.1	28.6	-1.6
4	16.4	21.4	11.3	8	6.51	49	36.4	1.4
5	20.6	25.7	15.3	9.8	5.22	34.3	41.7	6.7
6	25.3	30.7	19.7	11.4	2.56	11	44.8	11.1
7	28.6	34.2	22.8	11.8	0.53	4.4	45	14.8
8	28.4	34.1	22.8	11.3	0.55	4.3	44.6	13.6
9	25.3	31.2	19.5	9.8	1.71	16.9	42.5	10.3
10	20.6	26.6	15.3	7.9	5.45	70.9	41.2	4.9
11	15.5	21.3	10.9	6.3	7.49	129.7	33	0
12	11.7	16.7	7.7	4.9	11.91	256.1	25.4	-1.9
13	18.8	24.2	13.8	8.2	73.5	1053.4	45	-4.6

HT=highest temperature; LT=lowest temperature; AT=average temperature; AHT=average highest temperature; AMT=average minimum temperature; AST=average sunbathing time (hours); ANDR=average number of rainy days; MTRA=monthly total rainfall average (mm).

First, Preparation of Data Sets was performed., upland biomass density modelling was performed using Sentinel-2 (S2) and GEDI L4A data. In addition, GLO-30 Digital Elevation Model (DEM) data was also used for slope calculations. In the study, time series from 2019 to 2024, which is the temporal data intersection time of the layers, were used. In the study, the time series from 2019 to 2024, which is the temporal data intersection time of the layers, was used.

The datasets used in the study and their corresponding characteristics are presented in the Table.2 below. The process steps are as follows: Sentinel-2 data were filtered to the region and time interval specified for the year 2022. Then, various quality controls and band scaling operations were performed on the images. Besides, various vegetation and surface indices such as NDVI,

MNDWI, NDBI, EVI and BSI have been added. GEDI L4A data was used for biomass density estimations and improved with filters such as data quality and slope. Areas sloping more than 30 degrees were masked. Elevation and slope bands were calculated using DEM data and these data were added to the system as additional variables to be used in biomass estimation.

As the second step, Data Processing and Filtering process was performed. Quality control filters were applied on Sentinel-2 and GEDI data. For Sentinel-2 data, images with low cloudiness values were selected using 'Cloud Score Plus' and the spatial resolution of the images was scaled to 10 metres. GEDI data Quality was controlled with '14_quality_flag' and 'degrade_flag' variables and masked with variables such as slope and error rate. As the third step, Model Training process was performed.

Sentinel-2 and DEM data were used to model the biomass density to be estimated:

Random Forest regression algorithm was preferred for modelling biomass density. The model was trained to estimate the aboveground biomass density (AGBD) for each pixel. The training data was limited to 1000 samples and these samples were determined by stratified sampling method. In the training process, Sentinel-2 image bands and DEM bands were used as 'predictors' and GEDI data was included in the model as 'predicted' values.

As the fourth step, Model Evaluation process was performed. The performance of the model was evaluated using the root mean square error (RMSE). Furthermore, a scatter plot visualising the relationship between the predicted biomass density values and the observed values was created. In the graph, the predicted and

observed biomass values are compared and a linear trend line is added on the graph. As a result of this analysis, biomass density was estimated and Total AGB (Mg), which is the total amount of biomass in the identified land classes, was extracted. Graphs, results and explanations are given under the heading of findings below

As the fifth step, Findings process was performed. In order to examine the relationship between the biomass density values estimated on an annual basis in the time interval between 2019 and 2023 and the observed values, each year is considered separately. Figure 7. below shows a certain slope in the Regression line graph between Observed and Aboveground Biomass Density between 2019-2020. A linear relationship was found between the predicted Aboveground Biomass Density values (y-axis) and the Observed values (x-axis).

Table 2. Data sets

SENTINEL-2			
Resolution	Detail		
Consideral Consideration of the Consideration of th	13 bands (443–2190 nm), covering visible, NIR, red		
Spectral	edge, and SWIR regions.		
Radiometric	12-bit resolution, reflectance range 0-4095, enabling		
Radionletite	high sensitivity.		
	10 m:B2-B4 (Vis),B8 (NIR);20 m: B5-		
Spatial	B8A(RedEdge),B11-12(SWIR);60 m: B1, B9-B10		
	(Atmospheric).		
Temporal	Revisit time \sim 5 days, varies by weather and location.		
GEDI L4A employs an active LiDAR system operating in a			
single near-infrared wavelength band.			
Spectral	GEDI L4A uses active LiDAR in a single NIR band.		
Radiometric	16-bit resolution captures backscatter with high		
Radioniedic	accuracy for detailed vertical structure.		
Spatial	Footprint: \sim 25 m; spacing: 60 m nadir, \sim 600 m globally.		
Temporal	45-day revisit (ISS-dependent); limited global coverage		
Temporal	due to orbit.		
GLO-30 Digital Elevation Model-DEM			
Spectral	LiDAR wavelength: 1064 nm (NIR).		
Radiometric	16-bit precision ensures accurate LiDAR backscatter		
Radionicalic	measurement.		
Spatial	Footprint: \sim 25 m; spacing: 60 m nadir, \sim 600 m globally.		
Temporal	45-day revisit (ISS-dependent); coverage limited to		
Temporal	orbital track		

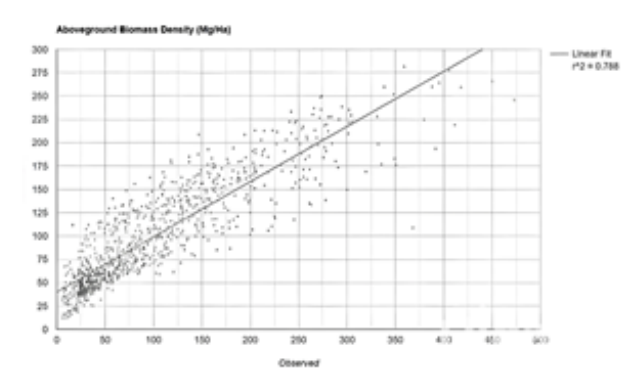


Figure 7. 2019-2020 regression graph.

R-square (r^2), 0.788 was obtained. This value reveals that the observed value, which is the independent variable of the model, explains the predicted biomass density, which is the dependent variable, at a high rate of 78.8%. Although the model cannot be called a perfect model, it is shown to be compatible with this value.

In satellite-based biomass estimation studies, numerous factors such as atmospheric effects, sensor noise, topographic variability, and vegetation diversity directly influence model performance. Despite these challenges, a high explanatory power of 78.8% ($R^2=0.788$) demonstrates both the statistical reliability and practical

applicability of the model. In this regard, the model provides a strong and reliable foundation for large-scale spatial biomass monitoring, offering a fast, scalable, and cost-effective approach.

The data are mostly distributed close to the regression line. This revealed the existence of a linear relationship. This graph reveals that the biomass density increases with increasing observed value. It has been observed that as the observed value increases, the deviations from the regression line increase. The 300-400 range is the range where this deviation is intense. A deviation from the regression line above 300 values was detected on the Observed (x-axis).

This reveals the deviation from the estimate. The reasons for this are also analysed and inferences are made. They will be explained in detail in the following sections of the study. The Regression line graph shows a certain slope in the same way as 2020-2021 shown in Figure. 8 below. A linear relationship was found between the predicted Aboveground Biomass Density values (y-axis) and Observed values (x-axis)

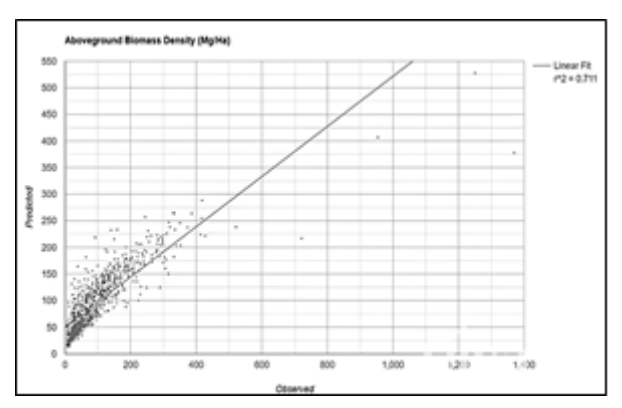


Figure 8. 2019-2020 Regression Graph.

R-square (r^2) , 0.793 was obtained. This value reveals that the observed value, which is the independent variable of the model, explains the predicted biomass density, which is the dependent variable, at a high rate of 79.3%.

Although the model cannot be called a high accuracy model, it is shown to be compatible with this value. The data mostly show a distribution close to the regression line. It has been revealed that these two variables change proportionally and there is a linear relationship. This graph reveals that biomass density increases with the increase in the observed value.

It was observed that as the observed value increased, the deviations from the regression line increased. While it is in harmony up to the range of 300-400, the deviations intensifies above 400. It has been determined that there are deviations from the model.

A significant deviation from the regression line was detected above 400 values of Observed (x-axis). In the observations after 500 values, these deviation values are at large rates. After these values, the model does not represent the observations well and reveals a bias away from the prediction. The reasons for this were also

analysed and inferences were made. They will be explained in detail in the following sections of the study. In the analysis for the years 2021-2022 shown in Figure 9 below, a linear relationship was found between the Estimated Above Ground Biomass Density values (y-axis) and the Observed (x-axis) values.

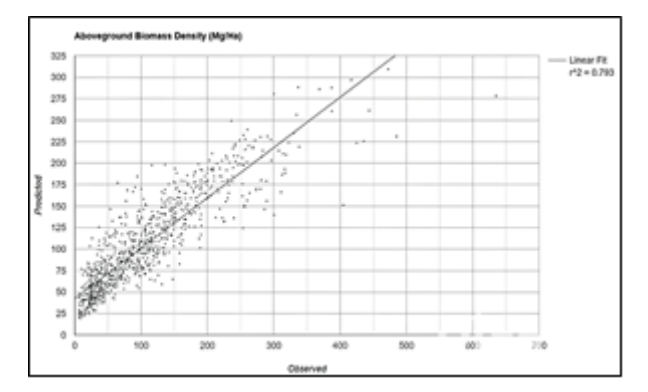


Figure 9. 2021-2022 Regression Graph.

R-square (r^2), 0.814 was obtained. This value reveals that the observed value, which is the independent variable of the model, explains the estimated biomass density, which is the dependent variable, at a high rate with a value of 81.4%.

The data was mostly close to the regression line. It was determined that the increase in biomass occurs when the amount of observation increases. While there is a distribution close to the regression line between 300-400, it was determined that the deviations from the model starting with the value of 400 and increasing with 500.

A linear relationship was found between the estimated Aboveground Biomass Density values (y-axis) and Observed values (x-axis) for the years 2022-2023 as shown in Figure 10 below.

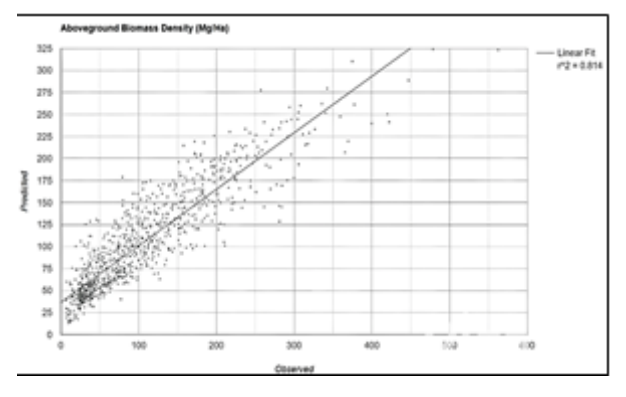


Figure.10. 2022-2023 Regression Graph.

R-square (r²), 0.711 was obtained. This value reveals that the observed value, which is the independent variable of the model, explains the predicted biomass density, which is the dependent variable, to a high extent with a value of 71.1%. The data were generally observed close to the regression line. It has been determined that The observed increase in biomass appears to correlate with increased sampling density The observed increase in

biomass appears to correlate with increased sampling density. Especially after the value of 600, anomalies were detected to a great extent.

R-square (r^2) , 0.711 was obtained. This value reveals that the observed value, which is the independent variable of the model, explains the predicted biomass density, which is the dependent variable, to a high extent with a value of 71.1%. The observed increase in biomass appears to correlate with increased sampling density. Especially after the value of 600, anomalies were detected to a great extent.

In the interpretation of the linear regression analysis graph between Observed and Aboveground Biomass Density between 2023-2024 shown in Figure 11 below, the following conclusions were obtained. A linear relationship was found between the predicted Aboveground Biomass Density values (y-axis) and the Observed values (x-axis).

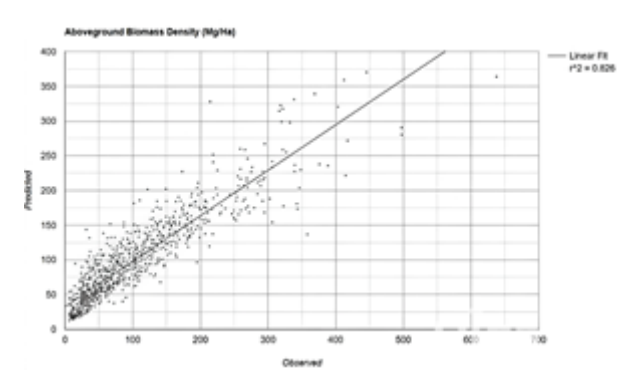


Figure.11. 2023-2024 Regression Graph.

R-square (r²), 0.826 was obtained. This value shows that the observed value, which is the independent variable of the model, explains the estimated biomass density, which is the dependent variable, to a high extent with a value of 82.6%. The distribution of the data is generally close to the regression line. As the amount of observations increases, the biomass increases. Especially after the value of 300, anomalies were detected to a great extent. In the study, Aboveground Biomass Density and the Root Mean Square Error RMSE value of the model were calculated separately for each year in the time interval from 2019 to 2024. The results obtained are shown in Table.3 below.

Table.3. Total AGB and RMSE by years

Time Interval	Total AGB(Mg)	RMSE
2019-2020	14043214.68	40.97
2020-2021	14638570.78	41
2021-2022	14339747.88	37.04
2022-2023	15029798.83	60.12
2023-2024	14658066.64	37.65

The following Figure.8. Annual Total AGB (Mg) graph was created by utilising the data in Figure.12 above. The lowest Total AGB(Mg) value in the study year range was

2019-2020 with the value 14043214.68, while the highest Total AGB(Mg) value was 2022-2023. A decrease was observed between 2023-2024, the last measurement interval

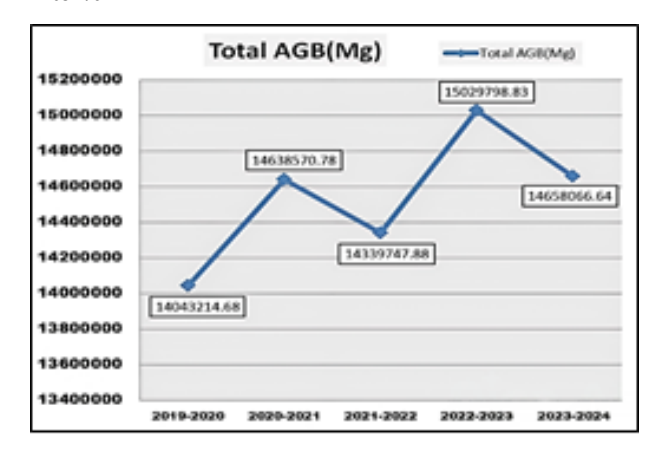


Figure.12. Total AGB by years.

The processes such as creating a data set for the study area, standardisation of the data, creating the data in the form of layers in the GIS platform environment, modelling the data, obtaining the estimated Total AGB (Mg) values were completed and the findings were obtained. In the light of these findings, discussion and conclusions are explained in detail below.

Increases in biomass observed over the years can be attributed to forest regeneration, insect outbreaks, land use changes, a decrease in wildfires, and post-fire forest restoration activities during these periods.

3. Results and Discussion

A negative situation such as climate change, soil degradation, soil erosion, urban growth, industrial pollution, decrease in water resources, decrease in biodiversity and natural disasters threaten the carbon sinks on the earth. With the decrease in these areas, diseases that threaten human health increase and living conditions become more difficult.

The reduction in forested areas is the most important variable that increases this amount. Forests are destroyed by harmful activities such as settlement, fires, conversion to agricultural land and stubble burning. In addition to being an indicator of negativity, forest enhancement activities in forests make a significant contribution to the increase in biomass in forest improvement activities. The study in the upper basin of the Göksu River in the Eastern Mediterranean found that the total above-ground stand carbon content increased by 47.6 thousand tons and this increase was achieved by forest improvement works (Günlü et al., 2019).

It was revealed that there will be a 6.62% decrease in plant biomass density in the study area Alanya until the end of 2030 in the projection of 2018 data (İşler et al., 2024). It has been determined that the region is under the threat of losing its natural carbon deposits due to urbanization pressure as well as climate change. The

common point in the studies reveals that urbanization pressure is associated with forest fires. The negative impact of urban growth pressure on vegetation was obtained due to the strong link between EVI and NDBI (Sharma et al., 2022; Zhang et al., 2004).

The transformation of green areas into urban areas, which can be characterized as irreversible actions in the ecosystem, or the negativities caused by human activities in urban areas reduce the biomass storage areas of the earth.

Tourism is an important economic income sector among human activities for the study area. Although this situation creates opportunities to increase economic income, it causes uncontrolled and unplanned urbanization and the reduction of natural land covers and natural landscape areas.

With this study, the change in Biomass Density in Alanya has been addressed in the year time interval. Forest above ground biomass (AGB) calculation with forecasting methodology was modelled with a dataset covering the time interval between 2019 and 2023 in order to guide local managers and planners. Spectral indices and bands data (Sentinel-2 Surface Reflectance) used as data set independent variable, cloudlessness mask (CloudScore+) due to the consideration of cloud factor to improve the quality of the data, Digital Elevation Model data (Copernicus GLO-30 DEM) containing Slope and Elevation information used as independent variables of the model, and Real-time Aboveground Biomass Density (GEDI L4A Raster Aboveground Biomass Density) data which is Raster data were included in the model in the study. This methodology demonstrates the applicability of AGBD estimation at both temporal and spatial scales using earth observation technology.

Global Ecosystem Dynamics Investigation (GEDI), produces Light Detection and Ranging (LIDAR) data with 60 m range and 30 m spatial resolution. The data obtains three-dimensional positional data of plants in the vertical direction. A solution was developed using the regression model, which is a machine learning method, as an indirect solution technique for converting point-based data into spatial data. In general, compared to other years, the 2023–2024 period experienced fewer wildfires and higher rainfall amounts. Therefore, the observed increase in aboveground biomass during this period can be attributed to these favorable environmental conditions.

In the application of the model over the years, the lowest Total AGB(Mg) value was 14043214.68 in the 2019-2020 time period and the highest Total AGB(Mg) value was 15029798.83 in the 2022-2023 time period. Here, the highest time interval was determined as the 2022-2023-time interval with the highest error value of RMSE value 60.12. For this reason, it was determined that additional variables should be included in the model in future studies.

In the modeling process, the Random Forest algorithm was used to capture nonlinear relationships between

variables. Its ability to reduce overfitting and provide high generalization performance makes it a prominent method. In comparison, Linear Regression is more effective for identifying linear relationships, while Support Vector Regression (SVR) can be less efficient on large datasets and is sensitive to parameter tuning. Random Forest was preferred in this study due to its flexibility, robustness, and ability to produce accurate results with minimal parameter configuration.

In this study, the hyperparameters of the Random Forest algorithm were selected manually. Instead of a systematic optimization approach, parameters were chosen using a trial-and-error-based method. This represents one of the key areas for improvement in future work.

With the model presented in this study, a feasible model with low image processing load but high accuracy has been presented.

In future studies to strengthen the model, it is suggested that adding new variables to the model by dividing it into subgroups such as humidity rate, soil type, plant species will reduce the amount of outline values in the model and increase the accuracy of the model. In the future, more diverse and rich studies can be produced by trying different regression models with linear regression models and new variables. There is a possibility that the approach of detecting complex relationships will make the model more powerful. After the findings that are suggestions for further studies, the fact that the model accuracy is close to high rates with the least variable input clearly reveals the success of the model in the study.

Since climate characteristics cause many effects on humans and nature, the subject of the study has emerged as an important variable in the decrease and increase of biomass. İşler et al. (2023) showed in their study that despite the population increase, biomass change is positive and the climate characteristics of the region have a positive effect on plant health. It has been found that the factors causing vegetation change are proportional to the relationship between urbanization and climate. It shows that climate conditions should be taken into consideration in determining positive proactive environmental planning and policies.

Another noteworthy result of the study is the emphasis on the critical role of the interaction between climate conditions and urbanization in shaping vegetation dynamics. In particular, despite higher levels of urbanization, Alanya exhibits a more favorable vegetation status, indicating the contribution of more favorable climatic conditions and positive proactive environmental policies.

Obtaining Total AGB(Mg) indirectly, which is difficult to obtain directly using Earth Observation technology, offers more practical and accurate solutions. Since it has become difficult to find biomass change with high accuracy due to economic and technical limitations, this methodology has provided decision makers and planners

with a solution-oriented contribution to the process by revealing the spatial and temporal biomass change of the region. In order to advance and develop the study, additional variables should be included in the model and studies should be carried out to improve the accuracy quality of opensource data.

Author Contributions

The percentages of the author' contributions are presented below. The author reviewed and approved the final version of the manuscript.

	E.A.	
С	100	
D	100	
S	100	
DCP	100	
DAI	100	
L	100	
W	100	
CR	100	
SR	100	
PM	100	
FA	100	

C=Concept, D= design, S= supervision, DCP= data collection and/or processing, DAI= data analysis and/or interpretation, L= literature search, W= writing, CR= critical review, SR= submission and revision, PM= project management, FA= funding acquisition.

Conflict of Interest

The author declared that there is no conflict of interest.

Ethical Consideration

Ethics committee approval was not required for this study because of there was no study on animals or humans.

References

- Aaslyng JM, Lund JB, Ehler N, Rosenqvist E. 2003. IntelliGrow: a greenhouse component-based climate control system. Environ Model Softw, 18(7): 657–666.
- Al Saud MM. 2022. Space techniques for earth observation. in: applications of space techniques on the natural hazards in the MENA Region, 1: 3–14.
- Askne JI, Dammert PB, Ulander LM, Smith G. 1997. C-band repeat-pass interferometric SAR observations of the forest. IEEE Trans Geosci Remote Sens, 35(1): 25–35.
- Cao L, Dubayah R, Zhang Z, Armston J. 2023. Validation of GEDI biomass estimates in Western U.S. forests using field inventory data. Remote Sens Environ, 295: 113630.
- Da Silveira F, Da Silva SLC, Machado FM, Barbedo JGA, Amaral FG. 2023. Farmers' perception of the barriers that hinder the implementation of agriculture 4.0. Agric Syst, 208: 103656.
- De Araujo V, Pramreiter M, Christoforo A. 2025. A global policy framework for the circular use of forest biomass as building materials. Nat Rev Mater, 3: 1–3.
- Duncanson L, Kellner JR, Armston J, Dubayah R, Minor DM, Hancock S, Healey S. 2022. Aboveground biomass density models for NASA's GEDI L2A data. Environ Res Lett, 17(9): 095001.

- Eckert S. 2012. Improved forest biomass and carbon estimations using texture measures from WorldView-2 satellite data. Remote Sens, 4(4): 810–829.
- Evrendilek F, Celik I, Kilic S. 2004. Changes in soil organic carbon and other physical soil properties along adjacent Mediterranean forest, grassland, and cropland ecosystems in Turkey. J Arid Environ, 59(4): 743–752.
- Foody GM, Cutler ME, McMorrow J, Pelz D, Tangki H, Boyd DS, Douglas IA. 2001. Mapping the biomass of Bornean tropical rain forest from remotely sensed data. Glob Ecol Biogeogr, 10(4): 379–387.
- Franklin J, Hiernaux PH. 1991. Estimating foliage and woody biomass in Sahelian and Sudanian woodlands using a remote sensing model. Int J Remote Sens, 12(6): 1387–1404.
- Gallaun H, Zanchi G, Nabuurs GJ, Hengeveld G, Schardt M, Verkerk PJ. 2010. EU-wide maps of growing stock and above-ground biomass in forests based on remote sensing and field measurements. For Ecol Manag, 260(3): 252–261.
- Gilreath JP, Jones JP, Overman AJ. 1994. Soil-borne pest control in mulched tomato with alternatives to methyl bromide. 156– 159.
- Günlü A, Göl C, Sariçam F. 2019. The evaluation of temporal and spatial change of aboveground stand carbon: a case study of upstream of the Göksu river basin. 352–359.
- Güverçin İ. 2022. Estimation of aboveground biomass in pure red pine stands using Sentinel-1A and Landsat 8 OLI satellite images (Anamur forest sub-district directorate example). PhD thesis, Çankırı Karatekin University, Institute of Science, Cankırı, pp. 65-66.
- Houghton RA, Hall F, Goetz SJ. 2009. Importance of biomass in the global carbon cycle. J Geophys Res Biogeosci. 114(G2).
- İşler B, Aslan Z, Sunar F, Güneş A, Feoli E, Gabriels D. 2023. Evaluation of prediction performance of vegetation biomass density for two different case study areas in Turkey with hybrid wavelet and artificial neural network method, pp:56-59
- İşler B, Aslan Z, Sunar F, Güneş A, Feoli E, Gabriels D. 2024. Hybrid model-based prediction of biomass density in case studies in Türkiye. Ecol Inform, 79: 102439.
- Keleş NN, Tepebaş B, Keleş S. 2024. Analysis of the temporal changes in the amount of carbon stored and oxygen produced in forest trees. Anat J For Res, 10(2): 16–21.
- Khan MN, Tan Y, Gul AA, Abbas S, Wang J. 2024. Forest aboveground biomass estimation and inventory: Evaluating remote sensing-based approaches. Forests, 15(6): 1055.
- Kim CK, Chung JD, Park SH, Burrell AM, Kamo KK, Byrne DH. 2004. Agrobacterium tumefaciens-mediated transformation of Rosa hybrida using the green fluorescent protein (GFP) gene. Plant Cell Tissue Organ Cult, 78: 107–111.
- Le Toan T, Beaudoin A, Riom J, Guyon D. 1992. Relating forest biomass to SAR data. IEEE Trans Geosci Remote Sens, 30(2): 403–411.
- Lu D, Batistella M. 2005. Exploring TM image texture and its relationships with biomass estimation in Rondônia, Brazilian Amazon. Acta Amazon, 35: 249–257.
- Muukkonen P, Heiskanen J. 2005. Estimating biomass for boreal forests using ASTER satellite data combined with standwise forest inventory data. Remote Sens Environ, 99(4): 434–447.
- Nelson R, Krabill W, Tonelli J. 1988. Estimating forest biomass and volume using airborne laser data. Remote Sens Environ, 24(2): 247–267.
- Potapov P, Li X, Hernandez-Serna A, Tyukavina A, Hansen MC, Kommareddy A. 2021. Mapping global forest canopy height through integration of GEDI and Landsat data. Remote Sens, pp: 52-58.

- Prentice IC, Farquhar GD, Fasham MJ, Goulden ML, Heimann M, Jaramillo VJ, Kheshgi HS, Le Quéré C, Scholes RJ, Wallace DW, Archer D. 2001. The carbon cycle and atmospheric carbon dioxide. In: Climate change 2001: The scientific basis. Intergovernmental Panel on Climate Change, pp:45-59.
- Protocol K. 1997. United Nations framework convention on climate change. Kyoto Protocol. Kyoto, 19(8): 1–21.
- Ravindranath NH, Ostwald M. 2007. Carbon inventory methods: handbook for greenhouse gas inventory, carbon mitigation and roundwood production projects. Springer, pp. 3.
- Sader SA, Waide RB, Lawrence WT, Joyce AT. 1989. Tropical forest biomass and successional age class relationships to a vegetation index derived from Landsat TM data. Remote Sens Environ, 28: 143–198.
- Santos JR, Freitas CC, Araujo LS, Dutra LV, Mura JC, Gama FF, Soler LS, Sant'Anna SJ. 2003. Airborne P-band SAR applied to the aboveground biomass studies in the Brazilian tropical rainforest. Remote Sens Environ, 87(4): 482–493.
- Sharma RK, Sankhayan PL, Hofstad O. 2008. Forest biomass density, utilization and production dynamics in a western Himalayan watershed. J For Res, 3: 171–180.
- Sharma V, Ghosh S, Singh S, Vishwakarma DK, Al-Ansari N, Tiwari RK, Kuriqi A. 2022. Spatial variation and relation of aerosol optical depth with LULC and spectral indices. Atmosphere, 13(12): 1992.
- Steininger MK. 2000. Satellite estimation of tropical secondary

- forest above-ground biomass: data from Brazil and Bolivia. Int J Remote Sens, 21(6-7): 1139–1157.
- Turgut R, Günlü A. 2022. Estimating aboveground biomass using Landsat 8 OLI satellite image in pure Crimean pine (Pinus nigra JF Arnold subsp. pallasiana (Lamb.) Holmboe) stands: a case from Turkey. Geocarto Int, 37(3): 720–734.
- Watson RT, Noble IR, Bolin B, Ravindranath NH, Verardo DJ, Dokken DJ. 2000. Land use, land use change, and forestry, pp:1-373.
- Zhang P, Liu H, Li H, Yao J, Chen X, Feng J. 2023. Using enhanced vegetation index and land surface temperature to reconstruct the solar-induced chlorophyll fluorescence of forests and grasslands across latitude and phenology. Front For Glob Change, 6: 1257287.
- Zhao P, Lu D, Wang G, Liu L, Li D, Zhu J, Yu S. 2016. Forest aboveground biomass estimation in Zhejiang Province using the integration of Landsat TM and ALOS PALSAR data. Int J Appl Earth Obs Geoinf, 53: 1–5.
- Zheng D, Rademacher J, Chen J, Crow T, Bresee M, Le Moine J, Ryu SR. 2004. Estimating aboveground biomass using Landsat 7 ETM+ data across a managed landscape in northern Wisconsin, USA. Remote Sens Environ, 93(3): 402–411.
- Zimble DA, Evans DL, Carlson GC, Parker RC, Grado SC, Gerard PD. 2003. Characterizing vertical forest structure using small-footprint airborne LiDAR. Remote Sens Environ, 87(2-3): 171–182.